Cassini Imaging Science: Initial Results on Phoebe and Iapetus

C. C. Porco, *et al.*

Science **307**, 1237 (2005);
DOI: 10.1126/science.1107981

Science (print ISSN 0036-8075; online ISSN 1095-9203) is published weekly, except the last week in December, by the American Association for the Advancement of Science, 1200 New York Avenue NW, Washington, DC 20005.

Cassini Imaging Science: Initial Results on Phoebe and Iapetus

C. C. Porco,[1*] E. Baker,[1] J. Barbara,[2] K. Beurle,[3] A. Brahic,[4] J. A. Burns,[5] S. Charnoz,[4] N. Cooper,[3] D. D. Dawson,[6] A. D. Del Genio,[2] T. Denk,[7] L. Dones,[8] U. Dyudina,[9] M. W. Evans,[3] B. Giese,[10] K. Grazier,[11] P. Helfenstein,[5] A. P. Ingersoll,[9] R. A. Jacobson,[11] T. V. Johnson,[11] A. McEwen,[6] C. D. Murray,[3] G. Neukum,[7] W. M. Owen,[11] J. Perry,[6] T. Roatsch,[10] J. Spitale,[1] S. Squyres,[5] P. C. Thomas,[5] M. Tiscareno,[5] E. Turtle,[6] A. R. Vasavada,[11] J. Veverka,[5] R. Wagner,[10] R. West[11]

The Cassini Imaging Science Subsystem acquired high-resolution imaging data on the outer Saturnian moon, Phoebe, during Cassini's close flyby on 11 June 2004 and on Iapetus during a flyby on 31 December 2004. Phoebe has a heavily cratered and ancient surface, shows evidence of ice near the surface, has distinct layering of different materials, and has a mean density that is indicative of an ice-rock mixture. Iapetus's dark leading side (Cassini Regio) is ancient, heavily cratered terrain bisected by an equatorial ridge system that reaches 20 kilometers relief. Local albedo variations within and bordering Cassini Regio suggest mass wasting of ballistically deposited material, the origin of which remains unknown.

Phoebe orbits Saturn at a distance of 12.9 × 10^6 km every 550 days in a retrograde orbit, which suggests that it was captured early in solar system history (*1*). The Cassini spacecraft flew within 2071 km of Phoebe to enable high-resolution remote-sensing observations and determination of the satellite's mass. Ground-based and low-resolution Voyager images had shown the satellite to be dark (normal reflectance ~0.08), with relatively small regions that were ~50% brighter (*2*). This dark surface has been hypothesized to be a source for material coating Iapetus, although it is known that Phoebe's surface is spectrally different from the dark material on Iapetus (*3*, *4*).

The Imaging Science Subsystem (ISS) (*5*) obtained images of Phoebe at better than 2 km pixel^{-1} (Fig. 1) over slightly more than three Phoebe rotations (period of 9.27 hours) (*6*); the closest approach occurred on 11 June 2004. The highest resolution images have a pixel scale of 13 m. We derived a spin-pole orientation of right ascension = 356.6°, declination = 77.9° from 211 control points measured in 80 images. The previous solution from Voyager data was only 9° different (*7*). Additional stereo solutions and matching limb and shadow positions provide a 2° by 2° digital model of the shape (*8*), from which the satellite's volume and major topographic forms can be measured. The mean radius is 106.6 ± 1 km. Phoebe's topography, relative to an equipotential surface, is within the range of other small objects and is much higher than that for clearly relaxed objects.

The calculated volume, 5.07 ± 0.14 × 10^6 km^3, combined with the mass determined from tracking the spacecraft (*9*), gives a mean density of 1630 ± 45 kg m^{-3}. The surface gravity on Phoebe, including rotational effects, ranges from 3.8 to 5.0 cm s^{-2}, and escape velocity, for objects launched vertically, ranges from 89 to 108 m s^{-1}.

Mean density is a function of both the sample density and the body's overall porosity. For porosities <~40%, Phoebe's mean density of 1630 kg m^{-3} requires a mixture of ice and rock of some type (Fig. 2). For porosities >~40%, Phoebe could be a completely rocky body. However, the identification of water ice on its surface telescopically (*10*, *11*) and evidence from the Cassini Visual and Infrared Mapping Spectrometer (VIMS) experiment (*12*) that shows widespread water ice, water of hydration, and trapped CO_2 on the surface suggest a more volatile overall composition. In addition, ISS images suggest icy materials at and near the surface. Furthermore, most examples of high inferred porosities, such as

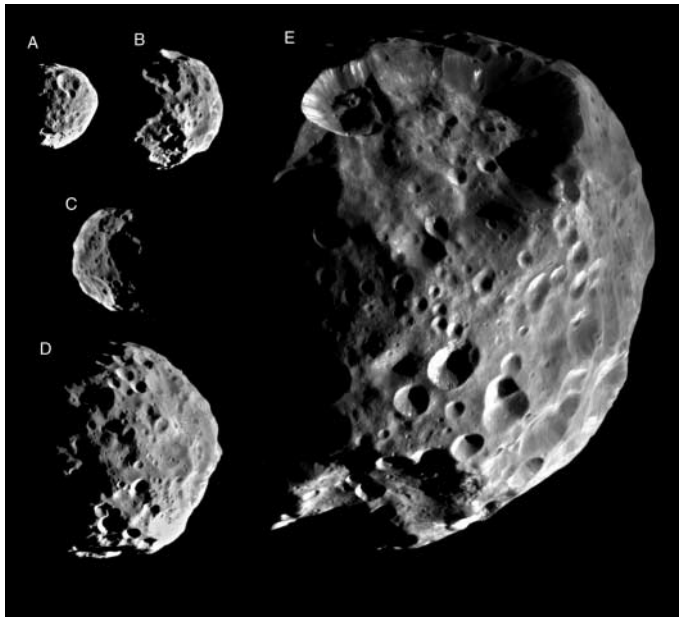

Fig. 1. Global views of Phoebe. (**A**) Image N1465644359, from 195,000 km, subspacecraft (S/C) longitude of 78°W. (**B**) N1465652463, 144,000 km, 165°W. (**C**) N1465700301, 160,000 km, 142°W. (**D**) N1465662798, 78,000 km, 276°W. (**E**) Mosaic of N1465669778 and N1465669953, 33,000 km, 349°W. Part of N1465669953 has been reprojected to match the limb of the other image. North is approximately up in all images.

[1]Cassini Imaging Central Laboratory for Operations, Space Science Institute, 4750 Walnut Street, Suite 205, Boulder, CO 80301, USA. [2]Goddard Institute for Space Studies, NASA, 2880 Broadway, New York, NY 10025, USA. [3]Astronomy Unit, Queen Mary, University of London, London, E1 4NS, UK. [4]Centre d'Etudes de Saclay, Université of Paris 7, L'Orme des Merisiers, 91191 Gif-sur-Yvette Cedex, France. [5]Department of Astronomy, Cornell University, Space Sciences Building, Ithaca, NY 14853, USA. [6]Department of Planetary Sciences, University of Arizona, 1629 East University Boulevard, Tucson, AZ 85721, USA. [7]Institut für Geologische Wissenschaften, Freie Universität, 12249 Berlin, Germany. [8]Department of Space Sciences, Southwest Research Institute, 1050 Walnut Street, Suite 400, Boulder, CO 80302, USA. [9]Division of Geological and Planetary Sciences, California Institute of Technology, 150-21, Pasadena, CA 91125, USA. [10]Institute of Planetary Research, German Aerospace Center, Rutherfordstrasse 2, 12489 Berlin, Germany. [11]Jet Propulsion Laboratory, California Institute of Technology, 4800 Oak Grove Drive, Pasadena, CA 91109, USA.

*To whom correspondence should be addressed. E-mail: carolyn@ciclops.org

the co-orbital moons, Janus and Epimetheus, and the F-ring shepherds, Pandora and Prometheus, occur for objects whose central pressures are exceeded below a few kilometers depth in Phoebe. Thus, Phoebe might not sustain such porosities over a large fraction of its volume.

For zero porosity, Phoebe's density would imply a mixture of ice and rock similar to those of the large icy satellites Ganymede, Callisto, and Titan (Fig. 2). Estimates of rock fractions for the smaller icy satellites (Mimas, Tethys, Dione, Rhea, and Iapetus) range from 0.25 to 0.5 (*13*), resulting in a range of sample densities from ~1100 to 1500 kg m^{-3}. Given that some porosity is plausible for a small satellite, Phoebe's sample density is thus probably greater than that found in the icy satellites of either Jupiter or Saturn but less than the mean densities of Pluto and Triton, objects thought to be representative of Kuiper Belt Objects, with implied rock fractions of about 0.7, or an equivalent sample density of ~1900 kg m^{-3} (*14*).

Phoebe's surface is dominated by impact craters, large landslides, and local albedo markings (Figs. 1 and 3). Phoebe's craters range in diameter from the lower limit imposed by the image resolution, ~50 m, to almost the maximum limit imposed by the size of Phoebe itself, ~100 km; there are >130 craters with diameters >10 km. The vast majority of Phoebe's craters have morphologies typical of simple craters seen throughout the solar system, including the usual range of forms apparently induced by subsequent mass movement or other impacts. Because of the low gravity on Phoebe, there should be no central-peaked or multiringed craters, and this is indeed the case.

Two craters exhibit large mass-movement accumulations (Figs. 1E and 3B). Hummocky debris on the floor of the 100-km crater named Jason (Fig. 4) probably originated from the north and east slopes, which are steep sided and exhibit evidence of recent downslope motion, including some bright streamers. Crenulations in the rim of a smaller crater named Erginus correlate with lobes of debris on the floor (Fig. 1E). The larger mass-movement accumulation in Jason has sections ~2 km thick, and its total volume is estimated to be >10^3 km^3. The current height of the eastern wall ranges from 11 to 15 km, with slopes up to ~40°. This wall could have supplied the estimated volume of slumped material with less than 2 km of horizontal retreat. The deposit within Jason may have been emplaced in several events, and the debris inside crater Erginus, which postdates some of the Jason landslides, may also consist of two or more discrete flows, one of which appears to have overtopped the crater's south rim.

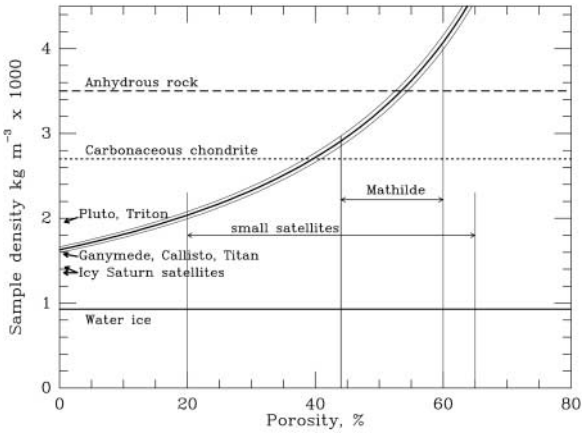

Fig. 2. Sample density for Phoebe as a function of porosity. For any given density, greater porosity requires a higher sample density. For Phoebe's mean density of 1630 kg m^{-3}, porosities less than 40% require some mixture of rock and ice; higher porosities could exist without an ice component. For comparison, calculated porosities of small, icy Saturn satellites range between 20% and 65%; asteroid Mathilde, a rocky object, has porosities as high as 60%.

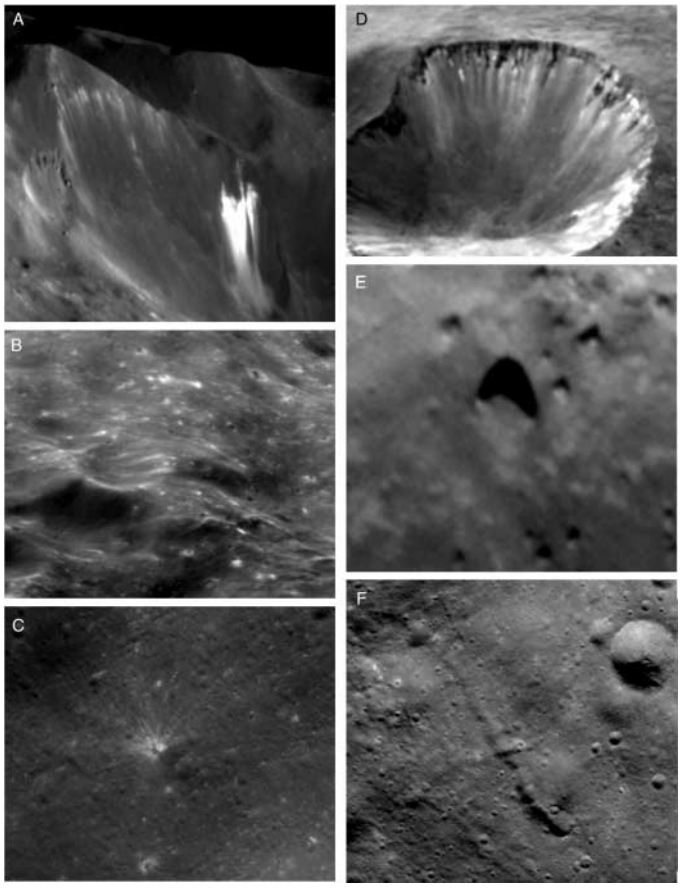

Fig. 3. Details of morphology of Phoebe. (**A**) Bright exposures and downslope streamers in Jason crater. Portion of N1465673138; image width 15 km; centered at 31°N, 302°W. (**B**) Bright markings surrounding small craters in hummocky material that probably was emplaced as landslides from the walls of crater Jason. Portion of N1465677447; image width 26 km; centered at 21°N, 318°W. (**C**) Crater with bright rays, and other craters exposing bright material. Portion of N1465674782; image width 8.2 km; centered at 1°N, 346°W. (**D**) Crater with banding in upper slopes. Portion of N1465672905; image width 17 km; centered at 36°S, 334°W. (**E**) Ejecta blocks in bottom of crater; largest is ~300 m across. Portion of N1465674693; image width 1.8 km; centered at 1°S, 353°W. (**F**) Elongate depression, possibly secondary crater chain. Portion of N1465674502; image width 10.5 km; centered at 0°N, 11°W.

Phoebe is a densely cratered object. Cumulative numbers of craters, between 100 m and 100 km diameter, per unit area, define a steep-sloped curve (Fig. 5). Crater densities approach those seen on other heavily cratered objects (*15*, *16*). This impact record may show the effects of impacts by other small, irregular saturnian satellites. Phoebe itself is the largest member of a group of at least five objects with similar inclinations and eccentricities (*17*, *18*). The population of irregular satellites should produce craters a few tens of kilometers in diameter (*17*, *19*). The high crater frequencies strongly suggest a surface at least 4 Gy old, consistent with early capture into Saturn orbit (*1*), when the outer solar system probably had a large population of small objects (*20*).

Photometric properties can help distinguish materials and geologic units. Cassini's encounter with Phoebe provided coverage in

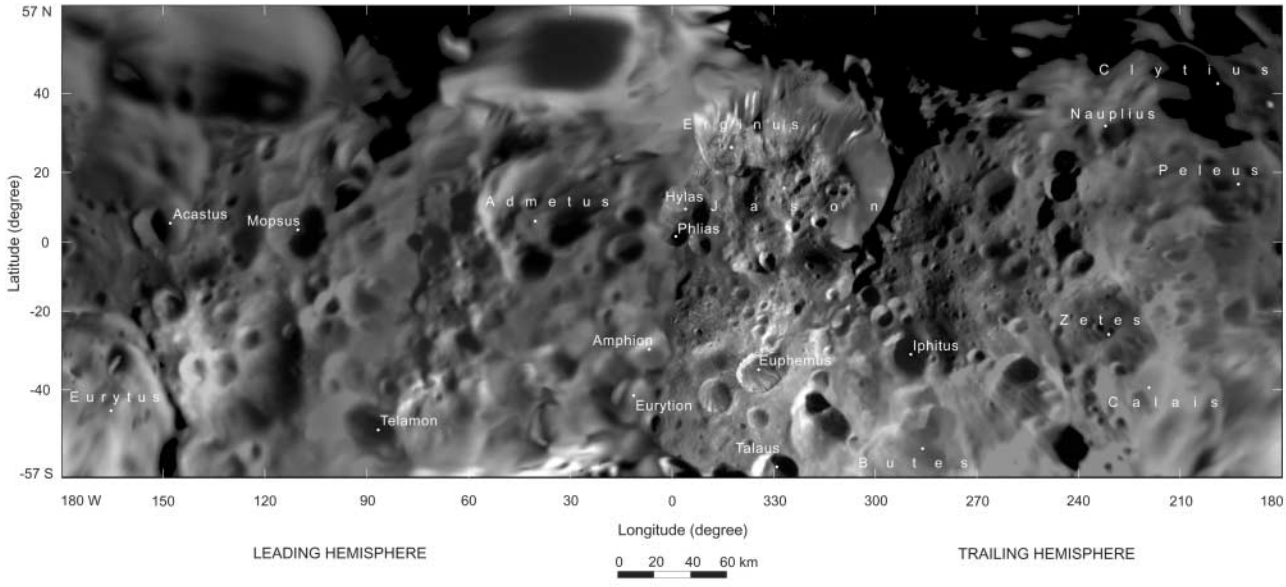

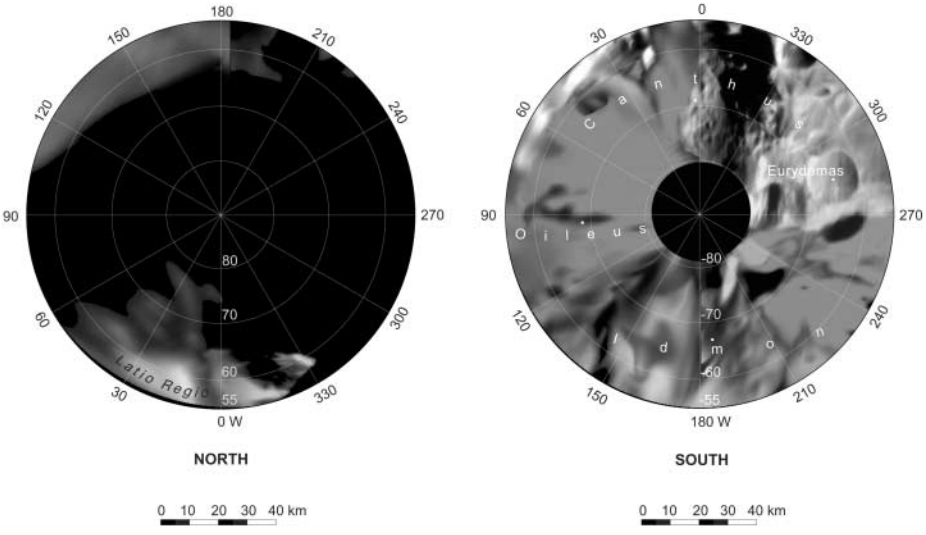

Fig. 4. A mosaic of images of Phoebe, including the provisional names assigned to some craters by the International Astronomical Union. South polar regions were imaged only at high emission angles; high northern latitudes were in darkness. Resolution and solar phase changed during flyby.

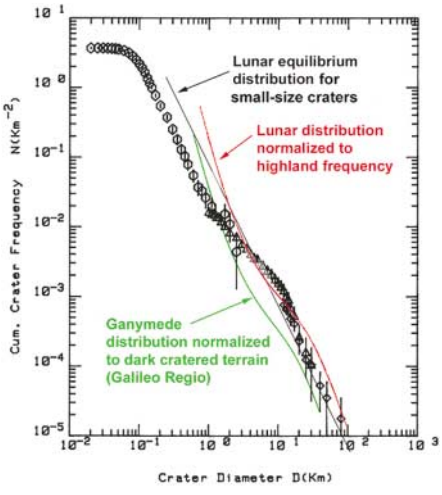

Fig. 5. Cumulative crater size-frequency distributions of Phoebe measured at image pixel scales from 4 km down to 30 m. The red curve is the lunar production function normalized to (average) lunar highland frequencies [see, e.g., (*35*)]. The green curve represents the production function derived for Jupiter's largest satellite, Ganymede, normalized to old, dark, cratered terrain of Galileo Regio (*16*, *36*). The shapes of the lunar and Ganymede production-function curve and the Phoebe crater size-frequency distributions at larger sizes all show departures from simple log functions. Also shown is the lunar equilibrium distribution with a –2 slope for small craters in the lunar maria (e.g., *16*).

solar phase angle (α) from 24° ≤ α ≤ 92°. Rotational light curves derived from the preflyby and postflyby data displayed no substantial variations of whole-disk color with longitude. At α near 90°, the average whole-disk brightness of Phoebe was about one magnitude brighter than expected by extrapolating the best-available Voyager photometric model (*2*). This discrepancy suggests that average regolith particles on Phoebe's surface scatter light more isotropically than predicted from the Voyager model, which was constrained only by data at α ≤ 33°.

We find a range of normal reflectances (r_n) of $0.07 \leq r_n \leq 0.3$. Local albedo variations on the surface of Phoebe having contrast factors of 2.0 to 3.0 as measured by ISS are manifested chiefly as brighter downslope streamers and bright annuli, rays, or irregular bright areas around small craters. Small parts of a few downslope streamers (Fig. 3A) are saturated in ISS images and thus have yet higher reflectances, but these represent a small fraction of the bright albedo features on Phoebe. These contrast ratios suggest normal reflectances of ~30% or less, values incom-

patible with clean ice. Thus, although most of the brighter outcrops are probably rich in ice, they are "dirty" (contaminant fraction could still be small) and could evolve to darker lag deposits that mantle Phoebe's surface through sublimation and thermal degradation processes related to insolation, sputtering, and impact cratering.

Bright material appears to be exposed by cratering on flat areas and gentle slopes and by mass wasting of steep scarps. Bright spots are associated with craters (Fig. 3, B and C) ranging from below the image resolution to ~1 km in size. Material excavated by impacts typically comes from depths <0.1 crater diameter (*18*); thus, the bright crater deposits represent material from a few meters to ~100 m in depth. Bright exposures also occur in landslide debris, which represents a mixture of materials from a variety of depths. Therefore, the brighter, ice-rich material occurs at shallow depths (or deeper) in widespread geographic and geologic settings. However, only a small fraction of craters, (<10%) in a limited size range (diameters <~1 km) presently displays bright materials. This observation suggests that bright materials darken or are covered as they age by processes such as infall of dark material from impacts among other small, outer satellites (*21*); deposition (regional or global) of debris excavated from elsewhere on Phoebe; sublimation of ice from the bright component; or, possibly, photochemical darkening of impurities in the brighter material.

The walls of some craters ranging from ~20 to 100 km in diameter (Fig. 3D) show evidence for layering or banding of materials at depth. In Jason (Fig. 3A), alignment of exposures of bright material suggests some layering at depths >1 km. The event that created Euphemus (Fig. 3D) may have excavated a layered surface, or the banding may represent exposure of the crater's own ejecta by slumping of oversteepened wall material near the rim.

Elongate depressions, typically less than 200 m wide and of varying continuity, are visible in some of the higher resolution images (Fig. 3F). Most of these are radially aligned with the overlapping craters Phlias and Hylas, near 0°W. The association suggests that these may be secondary craters, or fractures, or both, formed by the creation of a relatively young crater.

The presence of boulders 30 to 300 m across (Fig. 3E), collected in the bottoms of craters and scattered between craters, is fully

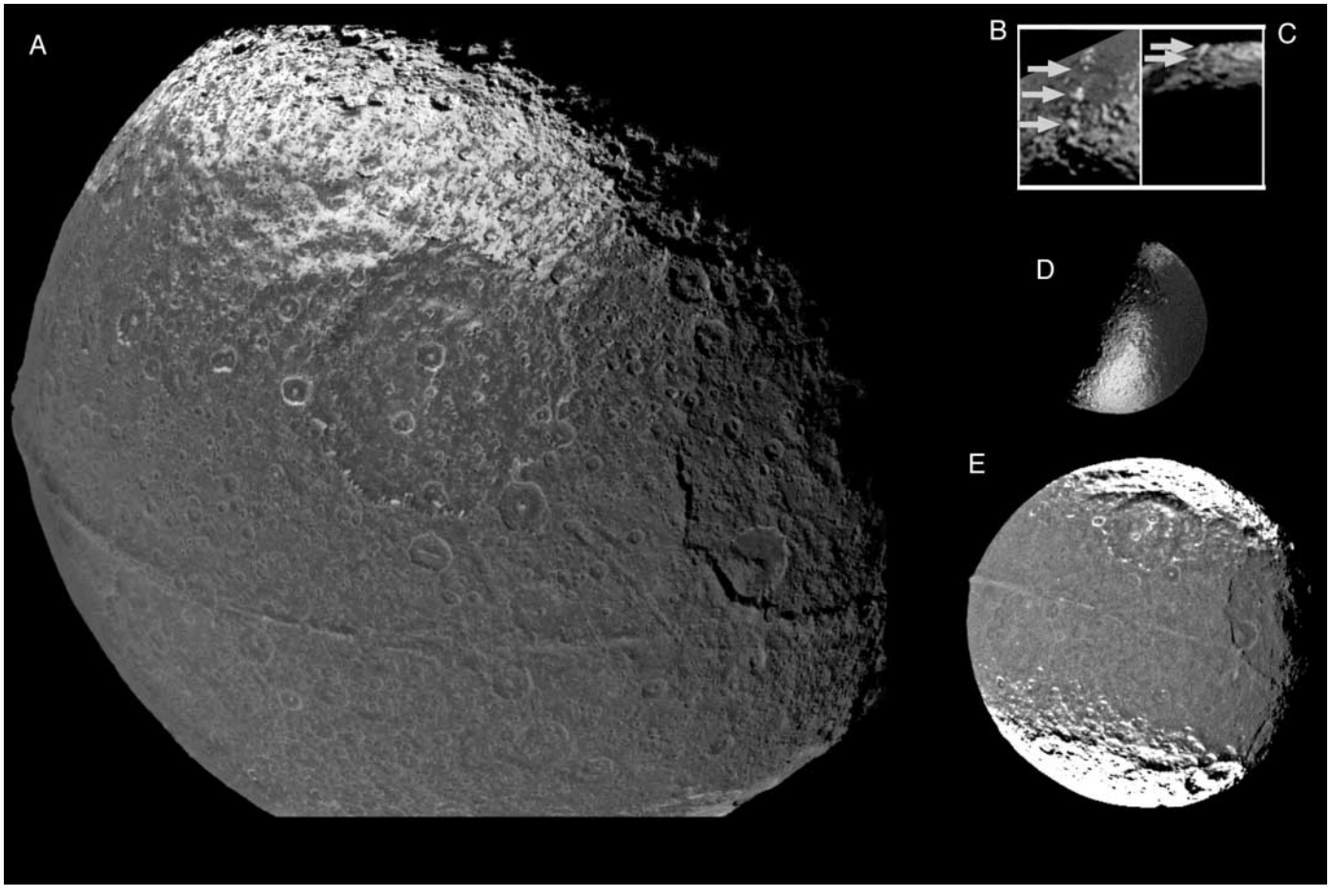

Fig. 6. Iapetus features. (**A**) Mosaic of images N1483151512, N1483152862, N1483152937, and N1483153026. The disk's middle is at 20°N, 80°W. The ridge runs roughly along 2°S and in this view traverses longitudes 40°W to 150°W, a distance of about 1400 km. Streaked dark markings in the brighter area at the top point back to the center of the leading side of Iapetus. Bright markings on the southern rim of the 400-km crater near the center indicate downslope motion and preferential exposure on north-facing slopes. (**B**) Detail of peaks along the equatorial ridge. Portion of image N1476735994, rotated; image edge at upper left; width is ~350 km. Peak near middle is at 1°S, 190°W. (**C**) Peaks seen on limb in image N1476993421, S/C = 7°S, 292°W. Peaks on limb are at ~205°W, essentially on the equator. North is to left. (**D**) View of linear chain of peaks at transition from Cassini Regio (right) to brighter terrain. Image N1476575655, S/C = 27°S, 216°W. Line of bright peaks extends from 185°W to 210°W and is within 2° of the equator. North is to upper right. Diameter of disk is ~1490 km. (**E**) Cassini Regio, bright polar areas, large basins, and equatorial ridge. Image N1482859934, S/C = 2°S, 70°W. North is to upper right. Basin on the right is ~550 km across; the one near the upper boundary of the dark area is 400 km across. Both basins show central raised structures, perhaps broad peak rings. A basin near the left limb (below equatorial ridge) is ~380 km diameter. Image has been contrast enhanced to show the features in the darker areas.

consistent with ejecta from cratering events. A 300-m block could have been produced by a ~25-km diameter crater (*22*). About 20 craters on Phoebe are between 25 and 50 km across.

Iapetus, Saturn's third-largest moon, orbits at a mean distance of 3.56×10^6 km on a slightly inclined prograde orbit. Cassini ISS obtained images of Iapetus during its first three orbits and during a flyby on 31 December 2004 with pixel scales that improve substantially on Voyager coverage. The most enigmatic feature of Iapetus from previous observations is the dark, roughly elliptical region centered on the leading side ("Cassini Regio") (*23*), darker by a factor of about 10 than parts of the trailing side (*24*). Theories for the origin of this feature have primarily involved the effects of impacts of material (exogenic theories), either by direct coating of the surface or by erosional effects of impacts (*3*, *25*–*29*). The source of possible impactors—whether the remnants of former cataclysmically disrupted satellites, or ejecta/dust from outer saturnian satellites like Phoebe, or interplanetary particles—has been uncertain. A possible internal (endogenic) origin has also been suggested (*30*) on the basis of dark markings beyond the contiguous dark area. Additionally, an origin by eruption of dark material, followed by deposition of brighter ice, followed by impact erosion has been proposed (*31*). Theories of formation by impacts (*26*) predict that albedo markings in craters and other topography near the edges of the dark area should be asymmetrically placed on topography because of grazing angles of impacts away from the apex of motion.

Cassini images show that Cassini Regio is heavily cratered, with at least three large impact structures with diameters >350 km. The region within ~20° latitude is, at the resolution of Cassini images, entirely darkened (except for slightly brighter crater rims), yet shows no obvious signs of volcanic flooding (Figs. 6 and 7). The largest basin is near 15°N, 30°W in the northeastern part of Cassini Regio (Fig. 6, A and E) and has a broad inner (peak) ring ~160 km in diameter. A 400-km basin is nearby, at 35°N, 80°W (Fig. 6, A and E), and a 380-km basin is on the anti-Saturn hemisphere near 15°S, 120°W. The latter structure has a somewhat polygonal outline and may have a central rise. A fourth large circular structure, ~500 km across, is detected within the bright terrain at ~45°S, 240°W in low-resolution (50 km pixel^{-1}) and high-phase (>110°) images. It, too, exhibits a central rise. These large craters have sizes, relative to Iapetus's size, consistent with the largest craters on other icy satellites. Smaller craters, tens of kilometers in diameter, show central peaks (Figs. 6A and 7B).

Crater counts have been carried out in two sets of images in the bright terrain at high southern latitudes. For crater diameters between 70 and 90 km, the crater frequencies measured in the Cassini ISS data are within a factor of ~1.5 of that found from earlier counts performed on Voyager data at a different location (*32*). This crater density confirms the old age of the bright part of the surface. Counts within the dark region are in progress. It is clear from visual inspection that it is also heavily cratered and thus old (Fig. 6A and Fig. 7, B to D). Whatever darkened the leading hemisphere of Iapetus postdated the formation of the craters within Cassini Regio.

Cassini images show substantial limb topography, relative to a reference sphere, that confirms earlier measurements from low-resolution Voyager images of unusually high topography for an object of this size (*33*). Cassini images from October 2004 captured several aligned peaks that had been identified in Voyager 2 images of the limb of Iapetus, on the anti-Saturn side, between ~185°W and ~215°W and within the dark terrain (Fig. 6, B to D). December 2004 images reveal that these aligned peaks are part of a near-equatorial ridge system that extends for more than 110° in longitude (Fig. 6, A and E, and Fig. 7, C and D). Parts of this ridge system rise more than 20 km above the surrounding plains, as determined from limb measurements. This ridge system includes sections that have sets of isolated peaks (Fig. 6, D to F), ridge segments more than 200 km in length, and

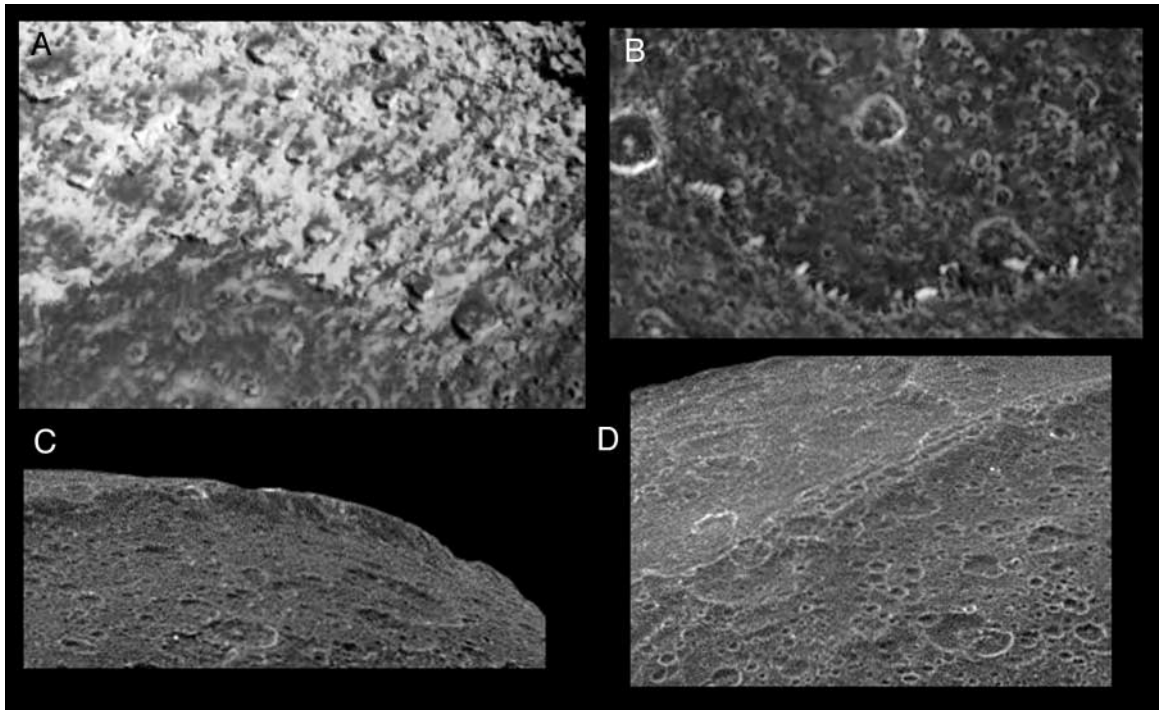

Fig. 7. Details of leading side of Iapetus. Contrast has been enhanced in all images. (**A**) Transition from Cassini Regio to polar region. Dark streaks follow trend from the center of Iapetus's leading side. Portion of image N1483173746; centered at 53°N, 74°W. North is approximately up in center of frame. (**B**) Bright streamers on north-facing slopes along rim of impact basin, bright crater rims, and some brighter central peaks. Portion of image N1483173746, centered at 25°N, 87°W, north approximately up. Bright streamers are visible on the north-facing slopes, bright crater rims, and some brighter central peaks of craters. (**C**) Equatorial ridge. Portion of N1483174305; center of ridge in this view is at 1°S, 50°W. View is ~200 km across. (**D**) Equatorial ridge. Portion of image N1483174398; centered at 3°S, 118°W. Ridge in some sections shows multiple parallel structures and many superposed impact craters.

some sections with three nearly parallel ridges. The ridge is cut by impact craters in some places, which indicates that it is not the most youthful surface feature (Fig. 7, C and D). The equatorial position of this feature suggests an origin related to the overall shape or changes in spin state of Iapetus. Iapetus is currently tidally locked into a synchronous 79-day spin. Internal energy losses will drive the bulge represented by the ridge, if not isostatically compensated, to lie along the equator, even if formed elsewhere relative to the body's spin vector (*33*). Despinning can cause complex tectonic patterns (*34*). However, the Iapetus ridge shows no characteristics or patterns comparable to the tectonic patterns seen in despinning models.

Some craters within the northern and southern transitional terrains between ~ 20° and 60° latitude show bright poleward-facing and dark equator-facing walls that are incompatible with the contrasts expected from the illumination conditions. This albedo polarity was noted in Voyager data (*29*), but Cassini images provide a higher resolution view of the albedo variations on those crater walls that exhibit this effect (Figs. 6A and 7). They show bright rims and central peaks of some craters within Cassini Regio and, in some instances, discrete downslope bright streamers occurring preferentially on north-facing slopes. An albedo asymmetry is continued into the brighter areas, where albedo variations are manifested chiefly as dark streaks on the brighter material, some associated with specific craters. The albedo contrasts make it difficult to discern the topographic outlines of many of the craters within the transition zone between ~40°N and 60°N. The orientations of the streaks away from the center of the leading side of Iapetus (which points in the direction of the apex of its orbital motion around Saturn) suggests deposition by some long-distance, ballistic transport of material (of either endogenic or exogenic origin), which either directly coated the surface of Iapetus and/or perhaps eroded or otherwise altered the pre-existing surface. The bright downslope markings on steeper crater walls, and the correlation of high albedo with regions of steeper slopes (e.g., crater rims and central peaks) within Cassini Regio indicate that the dark material is not thick (>1 km) deposits. These characteristics are consistent with some of the models of exogenic origin of Cassini Regio (*26*).

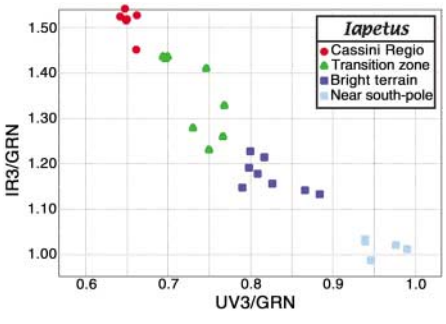

Fig. 8. Color-ratio diagram of locations on Iapetus taken at 54° phase angle; data from images N146837052, N1468370680, and N1468370800; spot sizes vary from 3 to 10 pixels across. Central wavelengths of the UV3, GRN, and IR3 color filters are 338, 568, and 930 nm, respectively. Data in the dark terrain are from 60°W to 140°W; high-latitude data are from 20°W to 150°W. The data's linear trend suggests mixing of two end members: Cassini Regio with a red spectrum and the south polar region with a flat spectrum.

Nonethess, the presence of a major geological feature of internal origin—the equatorial ridge—bisecting the leading hemisphere might suggest a genetic relationship between the ridge and the darkening of Cassini Regio. Such a relationship would require, to begin with, an internal heat source sufficient to drive eruptive volcanism extensive enough to cover an entire hemisphere. Although some degree of volcanism early in Iapetus's history might have been possible, there is no presently known heat source (such as conventional tidal heating) large enough for such extensive resurfacing of an entire hemisphere postdating the cratering epoch. Until a mechanism is found to generate substantial volcanic activity on Iapetus after the formation of its cratered surface, the Cassini evidence weighs in favor of an exogenic origin for Cassini Regio.

Data obtained through wide-band filters with central wavelengths between 380 nm and 930 nm (Fig. 8) show that there is a continuous range of colors between the darkest areas and the bright poles. Cassini Regio's color is uniformly red over 60° of longitude. Going south from the transition zone, the colors show a continuous progression of values to a nearly flat spectrum near the pole (Fig. 8). This behavior is consistent with spatial mixtures of two material end members, a dark non-ice and a bright water-ice component, at scales below the image resolution.

In summary, Phoebe is a body of rock and ice that exhibits an unexpected complexity of surface geology due to gravity-driven processes operating on a heavily cratered and compositionally heterogeneous surface. Iapetus's dark region is ancient, is bisected by a large equatorial ridge system, and shows evidence of ballistic emplacement of materials across its leading hemisphere.

References and Notes

1. J. A. Burns, in *Satellites*, J. A. Burns, M. S. Mathews, Eds. (Univ. Arizona Press, Tucson, 1986), pp. 117–158.
2. D. P. Simonelli *et al.*, *Icarus* **138**, 249 (1999).
3. T. C. Owen *et al.*, *Icarus* **149**, 160 (2001).
4. B. J. Buratti *et al.*, *Icarus* **155**, 375 (2002).
5. C. C. Porco *et al.*, *Space Sci. Rev.* **115**, 363 (2004).
6. J. M. Bauer, B. J. Buratti, D. P. Simonelli, W. M. Owen Jr., *Astrophys. J.* **610**, L57 (2004).
7. T. R. Colvin, M. E. Davies, P. G. Rogers, J. Heller, NASA STI/Recon. Tech. Rep. N-2934-NASA (1989).
8. Views of the shape models and other supporting materials are available on *Science* Online.
9. R. A. Jacobson *et al.*, *Bull. Am. Ast. Soc.* **35**, Abs. 15.02 (2004).
10. T. C. Owen *et al.*, *Icarus* **139**, 379 (1999).
11. M. E. Brown, *Astron. J.* **119**, 977 (2000).
12. R. N. Clark *et al.*, *Nature*, in press (2005).
13. G. Schubert *et al.*, in *Satellites*, J. A. Burns, M. S. Mathews, Eds. (Univ. Arizona Press, Tucson, 1986), pp. 224–292.
14. W. B. McKinnon, J. I. Lunine, D. Banfield, in *Neptune and Triton*, D. P. Cruikshank, Ed. (Univ. Arizona Press, Tucson, 1996), pp. 807–877.
15. G. Neukum, H. Dietzel, *Sci. Lett.* **12**, 59 (1971).
16. G. Neukum, B. A. Ivanov, in *Hazards Due to Comets and Asteroids*, T. Gehrels, Ed. (Univ. Arizona Press, Tucson, 1994), pp. 359–416.
17. D. Nesvorny, J. L. A. Alvarellos, L. Dones, H. F. Levison, *Astron. J.* **126**, 398 (2003).
18. B. Gladman *et al.*, *Nature* **412**, 163 (2001).
19. G. Neukum *et al.*, *Lunar Planet. Sci. Conf.* **29**, 1742 (1998).
20. J. M. Hahn, R. Malhotra, *Astron. J.* **117**, 3041 (1999).
21. H. J. Melosh, *Impact Cratering: A Geologic Process* (Oxford Univ. Press, New York, 1989).
22. P. C. Lee *et al.*, *Icarus* **120**, 87 (1996).
23. The Cassini Regio was named after the discoverer of Iapetus, Jean-Dominique Cassini.
24. D. Morrison *et al.*, *Icarus* **24**, 17 (1975).
25. D. P. Cruikshank *et al.*, *Icarus* **53**, 90 (1983).
26. J. F. Bell, D. P. Cruikshank, M. J. Gaffey, *Icarus* **61**, 192 (1985).
27. B. J. Buratti, J. Mosher, *Icarus* **115**, 219 (1995).
28. R. G. Tabak, W. M. Young, *Earth Moon Planets* **44**, 251 (1989).
29. T. Denk, G. Neukum, *Lunar Planet. Sci. Conf.* **31**, 1660 (2000).
30. B. A. Smith *et al.*, *Science* **215**, 504 (1982).
31. P. D. Wilson, C. Sagan, *Icarus* **122**, 92 (1996).
32. T. Denk *et al.*, *Lunar Planet. Sci. Conf.* **31**, 1596 (2000).
33. S. J. Peale, in *Planetary Satellites*, J. A. Burns, Ed. (Univ. Arizona Press, Tucson, 1977), pp. 87–112.
34. J. B. Pechman, H. J. Melosh, *Icarus* **38**, 243 (1979).
35. G. Neukum, B. A. Ivanov, W. K. Hartmann, in *Chronology and Evolution of Mars*, W. K. Hartmann, J. Geiss, R. Kallenbach, Eds. (Kluwer, Dordrecht, Netherlands, 2001), pp. 53–86.
36. G. Neukum, in *The Three Galileos: The Man the Spacecraft, the Telescope*, C. Barbieri, J. H. Rahe, T. V. Johnson, Eds. (Kluwer, Dordrecht, Netherlands, 1997), pp. 201–212.
37. We acknowledge the individuals at CICLOPS and across the Imaging Team who helped in planning and designing the Phoebe and Iapetus sequences and in keeping the imaging operations running smoothly. This paper is dedicated to the memory of Damon Simonelli, who developed much of the pre-Cassini understanding of Phoebe's surface. This work has been funded by NASA/Jet Propulsion Laboratory, the UK Particle Physics and Astronomy Research Council, the German Aerospace Center (DLR), and Université Paris VII Denis Diderot, Commissariat à l'Energie Atomique, Astrophysique Interactions Multiechelles, France.

Supporting Online Material

www.sciencemag.org/cgi/content/full/307/5713/1237/DC1
Figs. S1 and S2

29 November 2004; accepted 12 January 2005
10.1126/science.1107981